Cortical Morphometric Vulnerability to Generalized Epilepsy Reflects Chromosome- and Cell Type-specific Transcriptomic Signatures

Running title: Transcriptional signatures in generalized epilepsy

Jiao LI[1,2,3], Simon S. KELLER[4], Jakob SEIDLITZ[5,6], Huafu CHEN[1,2,3,✉], Bing LI,[1,3], Yifei WENG[7,8], Yao MENG[1,3], Siqi YANG[1,3], Qiang XU[7], Qirui ZHANG[7], Fang YANG[9], Guangming LU[7], Boris C. BERNHARDT[10], Zhiqiang ZHANG[7,✉], Wei LIAO [1,3,✉]

[1] The Clinical Hospital of Chengdu Brain Science Institute, School of Life Science and Technology, University of Electronic Science and Technology of China, Chengdu 611731, P.R. China.

[2] The Center of Psychosomatic Medicine, Sichuan Provincial Center for Mental Health, Sichuan Provincial People's Hospital, University of Electronic Science and Technology of China, Chengdu 611731, P.R. China.

[3] MOE Key Lab for Neuroinformation, High-Field Magnetic Resonance Brain Imaging Key Laboratory of Sichuan Province, University of Electronic Science and Technology of China, Chengdu 611731, P.R. China.

[4] Department of Pharmacology and Therapeutics, Institute of Systems, Molecular and Integrative Biology, University of Liverpool, UK.

[5] Children's Hospital of Philadelphia, Department of Child and Adolescent Psychiatry and Behavioral Science, Philadelphia, PA, USA.

[6] Department of Psychiatry, University of Pennsylvania, Philadelphia, PA, USA.

[7] Department of Medical Imaging, Jinling Hospital, Nanjing University School of Medicine, Nanjing 210002, P.R. China.

[8] Department of Radiology, The First Affiliated Hospital of Xiamen University, Xiamen 361001, P.R. China.

[9] Department of Neurology, Jinling Hospital, Nanjing University School of Medicine, Nanjing 210002, P.R. China.

[10] Multimodal Imaging and Connectome Analysis Laboratory, McConnell Brain Imaging Centre, Montreal Neurological Institute and Hospital, McGill University, H3A2B4 Montreal, Canada.

✉ Corresponding authors:

Huafu Chen (chenhf@uestc.edu.cn), The Center of Psychosomatic Medicine, Sichuan Provincial Center for Mental Health, Sichuan Provincial People's Hospital, University of Electronic Science and Technology of China, Chengdu 611731, P.R. China.

Wei Liao (weiliao.wl@gmail.com), The Clinical Hospital of Chengdu Brain Science Institute, School of Life Science and Technology, University of Electronic Science and Technology of China, Chengdu 611731, P.R. China.

Zhiqiang Zhang (zhangzq2001@126.com), Department of Medical Imaging, Nanjing Jinling Hospital, 305#, Eastern Zhongshan Rd., Nanjing 210002, P.R. China. Fax: +86-25-84804659. Tel: +86-25-84804659.

Word count of abstract: 225
Word count of main text: 4977
Number of Table(s): 1
Number of Figure(s): 4
Supporting Material (s): 1

Key points

- The morphometric similarity network (MSN) decreased in generalized epilepsy in the prefrontal, primary motor, and temporal areas; whereas it increased in the occipital, insular, and posterior cingulate cortices.
- Neuronal cells mostly contributed to the transcriptomic relationship of MSN differences in generalized epilepsy.
- MSN-related genes were specifically enriched for genes differentially regulated in previous studies of epilepsy but not of other brain disorders.

Abstract

Aims: Generalized epilepsy is thought to involve distributed brain networks. However, the molecular and cellular factors that render different brain regions more vulnerable to epileptogenesis remain largely unknown. We aimed to investigate epilepsy-related morphometric similarity network (MSN) abnormalities at the macroscale level and their relationships with microscale gene expressions at the microscale level.

Methods: We compared the MSN of genetic generalized epilepsy with generalized tonic-clonic seizures patients (GGE-GTCS, n = 101) to demographically-matched healthy controls (HC, n = 150). Cortical MSNs were estimated by combining seven morphometric features derived from structural magnetic resonance imaging for each individual. Regional gene expression profiles were derived from brain-wide microarray measurements provided by the Allen Human Brain Atlas.

Results: GGE-GTCS patients exhibited decreased regional MSNs in primary motor, prefrontal, and temporal regions, and increases in occipital, insular, and posterior cingulate cortices, when compared to the HC. These case-control neuroimaging differences were validated using split-half analyses and were not affected by medication or drug response effects. When assessing associations with gene expression, genes associated with GGE-GTCS-related MSN differences were enriched in several biological processes, including “synapse organization”, “neurotransmitter transport” pathways, and excitatory/inhibitory neuronal cell types. Collectively, the GGE-GTCS-related cortical vulnerabilities were associated with chromosomes 4, 5, 11, and 16, and were dispersed bottom-up at the cellular, pathway, and disease levels,

which contributed to epileptogenesis, suggesting diverse neurobiologically relevant enrichments in GGE-GTCS.

Conclusions: By bridging the gaps between transcriptional signatures and *in vivo* neuroimaging, we highlighted the importance of using MSN abnormalities of the human brain in GGE-GTCS patients to investigate disease-relevant genes and biological processes.

Keywords: cell-type-specific transcription; chromosome-specific transcription; genetic generalized epilepsy; morphometric similarity network; regional gene expression.

Introduction

Epilepsy is a chronic neurological disorder that affects over 70 million people worldwide [1]. The manifestations of epilepsy are spontaneous and recurrent epileptic seizures that occur in the brain [2]. Generally, genetic generalized epilepsy (GGE), which accounts for 15-20% of all epilepsies, has normal-appearing brain magnetic resonance imaging (MRI) [3]. However, *in vivo* neuroimaging has facilitated the identification of diverse scales of regional and connectomic alterations associated with epilepsy, and has revealed widespread and distributed changes [4-11].

Emerging evidence has shown subtle brain morphology/volume changes in GGE, but these findings have been controversial. Considering the thalamus, patients with GGE have been reported to have increased [12], decreased [7, 8], or no marked thalamic abnormalities [13]. Several studies have also reported cortical thinning [7-9], but the effects may be subtle [13, 14]. A large-scale international sample of epilepsy (n > 2,000) patients reported reduced volumes of the right thalamus and thinner bilateral precentral gyrus in GGE [8]. These variable findings may be due to the use of different methodologies or alternative multi-contrast MRI variables [15].

In contrast to using a single MRI variable for detecting structural brain abnormalities, morphometric similarity network (MSN) analysis combines multiple modalities or features that may provide insights into macroscale cortical organization in a single individual [16]. It has been shown that MSN may have close associations with cytoarchitectural classes, distinguished by cortical lamination patterns when compared with diffusion-weighted imaging tractography [16]. Furthermore,

abnormalities of the MSNs in mental diseases have been reported to be associated with regional brain gene expression patterns [17, 18], and may identify transcriptomic and cellular profiles of regional brain vulnerabilities to neurogenetic disorders [19]. Although the use of the MSN is a reliable and robust approach, it has not yet been used to identify brain network abnormalities in GGE, with clinical correlates of the disorder.

A predominant genetic contribution to GGE has been suspected. Overall, the percentage of epilepsy in siblings of patients with GGE is approximately 8%, suggesting the contribution of multiple gene variants [3, 20, 21]. Subsequent genome-wide association studies (GWAS) have implicated a number of common genes or loci with GGE [22, 23]. Although GWAS identified specific DNA variants that were responsible for these effects, multiple other factors could influence transcriptional activity and the ultimate abundance of proteins. Brain-wide gene expression atlases such as the Allen Human Brain Atlas (AHBA) microarray dataset [24] bridge the gap between human transcriptomes and neuroimaging [25]. Combining neuroimaging and transcriptomics may provide insight into how microscale architecture variations may relate to macroscale patterns of morphological alterations in various brain disorders [17-19, 26, 27]. In a recent study, Altmann *et al.* [28] identified over 2,500 genes overexpressed in regions of reduced cortical thickness across all epilepsies. These overexpressed genes showed enrichment for genes related to microglia and inflammation. Although GGE is a type of network disorder, the molecular and cellular mechanisms underlying distinctive regions of vulnerable and other preserved areas of multiple MRI features-based MSN in GGE are largely unknown.

In this study, we linked post-mortem gene expression information with *in vivo* structural imaging to identify molecular and cellular signatures of regional vulnerabilities to GGE-GTCS. We began by using the regional MSN method to test the dysconnectivity of patients with GGE-GTCS. We mapped case-control MSN differences at nodal levels and tested for significant differences in network organization across individuals. We then identified the relationships between regional MSN values and clinical factors in patients with GGE-GTCS. We next performed a functional enrichment analysis to identify the ontological pathways of genes associated with case-control regional MSN differences. Finally, we linked abnormal regional MSN-related genes to chromosomes and cell types to identify contributions to the transcriptomic relationships of GGE-GTCS-related changes in MSN.

Materials and Methods

Participants

Patients with GGE-GTCS (n = 114) and healthy controls (HC, n = 157) were enrolled at Jinling Hospital, Nanjing University School of Medicine, Nanjing, China. All study protocols were performed according to the Helsinki Declaration of 1975 and approved by the local Institutional Review Board. Written informed consent was obtained from all participants. Epilepsy diagnoses were performed by two experienced neurologists using analyses of clinical and imaging information, according to the guidelines of the International League Against Epilepsy classification [29]. The patients had typical seizure semiology of GTCS without precursory symptoms of partial epilepsy and aura, and generalized spike-and-wave discharges, using electroencephalogram analyses. No

patients had any remarkable abnormality on structural MRI visual reading. Moreover, patients were excluded because of i) progressive diseases, malformations of cortical development, tumours, or previous neurosurgery, or ii) incomplete MRI scanning. In addition, HCs had no history of neurological disorder or psychiatric illnesses, and no gross abnormality, as determined using structural MRI.

Data acquisition and data pre-processing

All patients with GGE-GTCS and HC underwent scanning using a Siemens 3.0 T MRI scanner (Siemens Medical Solutions, Erlangen, Germany) at Jinling Hospital, Nanjing, China. The structural images were acquired from a high resolution, T1-weighted (T1w) magnetization-prepared rapid gradient echo sequence (repetition time = 2,300 ms, echo time = 2.98 ms, flip angle = 9°, field of view = 256 × 256 mm^2, in-plane matrix size = 256 × 256, voxel size = 1 × 1 × 1 mm^3, and slices = 176).

The three-dimensional T1w images were pre-processed in surface-based space using FreeSurfer (version 6.0, http://surfer.nmr.mgh.harvard.edu/). Briefly, the cortical surface was reconstructed using skull stripping, segmentation of brain tissue, separation of hemispheres and subcortical structures, and construction of the grey/white interfaces and the pial surfaces [16, 30].

Construction of the MSN

The cortical surfaces were divided into 308 spatially contiguous regions [16-18, 31] derived from the original 68 cortical regions in the Desikan-Killiany (D-K) atlas [32]. This parcellation produced approximately equal sizes (~500 mm^2) for each region,

using a backtracking algorithm [31], which minimized the influence of variabilities in parcel sizes [16-19, 33]. This parcellated D-K atlas was transformed to each participant's surface to obtain an individual surface parcellation [16-18]. Seven features from the T1w images were extracted for each region, including surface area, cortical thickness, grey matter volume, intrinsic (Gaussian) curvature, mean curvature, curved index and folding index. Each participant's morphometric feature vector was *Z*-scored across cortical regions to account for variations in value distributions between features [16, 17]. Pearson's correlation analysis was performed on the morphometric feature vector between each paired cortical region, forming a 308 × 308 MSN for each participant. The procedures for constructing MSNs are shown in Fig. 1A.

Case-control comparisons of regional MSN

Regional MSN strengths were equivalent to the sum of the weighted degree (i.e., strength) of a given region to all other regions [16, 18]. To determine the distribution of the regional MSN, regional MSN strengths were averaged across all HC or patients with GGE-GTCS. In addition, to estimate case-control differences, we used a general linear model with age, sex, and total intracranial volume (TIV) as covariates. For each region i, the following model was used as: MSN_i ~ intercept + β_1×(Dx) + β_2×(age) + β_3×(sex) + β_4×(TIV), where Dx is the binary classification of GGE-GTCS patients and HC [19]. This model yields T- and P-values for the effect of case-control differences. To control type I error, the statistical significance was set at $P < 0.05$ with a false-discovery ratio (FDR) correction for multiple comparisons across 308 regions.

Statistical analyses

Demographic and clinical characteristics were evaluated between patients with GGE-GTCS and the HC. Age differences, TIV, and image quality were analysed using two-sample *t*-tests for normally-distributed variables and the Mann-Whitney *U*-test for non-normally distributed variables. Normality was assessed using D'Agostino-Pearson's omnibus normality test. The χ^2 test was used to assess sex differences. The statistical significance was set at $P < 0.05$.

Relationship between regional MSN and clinical variables

To investigate the clinical relevance of the MSN in GGE-GTCS, we correlated the clinical variables (duration of epilepsy and seizure frequency) with regional MSNs in altered cortical regions. Exploratory correlation analyses were also performed across all D-K 308 cortical regions. Partial correlation analyses were used to control for age as a confounding variable. The statistical significance was set at $P < 0.05$.

Transcriptional correlates of case-control regional MSN

We compared the case-control MSN map with post-mortem gene expression data from the AHBA ("Complete normalized microarray datasets", https://human.brainmap.org/static/download) [24] collected from six individuals at multiple brain anatomical locations. Pre-processing of the AHBA dataset followed an established pipeline [34]. Because the AHBA dataset included only two right hemisphere data, only the left hemisphere was considered in our analyses. Thus, a mean of all samples in a region was calculated to obtain the matrix (152 regions × 10,027 gene expression levels) of transcriptional level values [18].

Partial least squares (PLS) correlation [35], an explorative analysis, was used to correlate the case-control regional MSN patterns with the spatial distribution of transcriptional activities. Gene expression data were used as predictor variables of regional changes in MSN using PLS analyses. The first component of PLS (PLS1) was the linear combination of the weighted gene expression scores with a cortical expression map correlated with the case-control *t*-map of the regional MSN. To test whether the PLS1 explained more variance than expected by chance, we used a spin permutation test based on spherical rotations to account for spatial autocorrelation [36, 37]. First, we randomly permuted the rows (regions), preserving the spatial covariance structure regions (see below for the *Spin test*) in the gene expression matrix. We then compared the variance explained by the PLS correlation of the regional MSN differences on the observed transcriptional data with the distribution of variance in the difference of regional MSN explained by 5,000 random spin permutations. Finally, the P_{spin} values were obtained by comparing the observed variance explained to the centiles of the spin permutation distribution [18]. To examine the variability of each gene's weighting coefficient, we used a bootstrapping method (resampling with replacement of the 152 cortical regions) in the PLS analysis. The ratio of the observed weight coefficient of each gene to its bootstrap standard error was used to calculate the *Z*-scores of each gene weight on PLS1 [17, 18, 33, 38-40]. The set of significant genes was set at $P < 0.05$, after being FDR corrected. The PLS1 significant gene list is shown in Dataset S1.

Enrichment analysis

We tested whether the significant gene list shared enriched biological pathways with risk genes for GGE obtained from the previous GWAS studies using either meta- and

mega-analysis or whole-exome sequencing, and data reported from systematic reviews [22, 23, 41-44]. Metascape analysis (https://metascape.org/) provided automated meta-analysis tools to understand either common or unique pathways in 40 independent knowledge bases [45]. A multi-gene-list meta-analysis was performed to facilitate the understanding of pathways (and pathway clusters) that were shared between, or selectively ascribed to, specific gene lists. Routine comparative approaches included using Venn diagrams to identify hits that were common or unique to gene lists. However, when multiple gene lists were analysed, the identification of consistent underlying pathways or networks was more critical, because previous studies have reported that overlap between OMICs datasets was more readily apparent at the level of pathways or protein complexes [46, 47]. Thus, the PLS1+ significant gene list and risk genes from previous studies in individuals with epilepsy were submitted to the Metascape website to compare an arbitrary number of gene lists across both gene identities and ontologies with minimum overlap: 3, *P* value cut-off: 0.01, and minimum enrichment: 1.5 against a background of 20,232 brain-expressed genes. The background gene list was calculated after probe to gene re-annotation [34] and shown in Dataset S2. According to the Re-annotator toolkit [48], 45,821 probes out of 58,692 probes can be uniquely mapped onto a gene and could be related to an entrez ID. As a result, the re-annotated set of 45,821 probes corresponded to 20,232 unique genes. In addition, considering the various numbers of background genes, we used a more restricted list of background genes (16,831 genes) where probes exceed the background in at least 20% of the samples to perform the second set of enrichment analyses. All obtained pathways were thresholded at $P < 0.05$, FDR-corrected [49].

To test whether chromosomal gene expression was related to case-control regional MSN values, we assessed the chromosomal enrichment of the genes from PLS1. A median rank-based approach was used to evaluate the enrichment of gene lists for specific chromosomes 1:22 [19, 39]. We first ranked each gene in terms of its *Z*-score weighting on the PLS1. We then calculated the observed median rank for genes located on specific chromosomes. The second step of randomly selecting and ranking genes was repeated 5,000 times to sample the permutation distribution of median rank in each chromosome. The null hypothesis was that the observed median rank (for the genes located on each chromosome) was not significantly different from the median rank of a random list of genes (equivalent number of genes located on a given chromosome). Finally, the P_{perm} values of chromosomal enrichment genes were estimated by comparing the observed median rank to the centiles of null median rank distribution for each chromosome [19, 39]. The statistical significance was set at P_{perm} <5th or >95th centile.

To obtain gene sets for each cell type, we compiled data from five different single-cell studies using post-mortem cortical samples of human postnatal participants [19]. This approach avoided bias based on acquisition methodology, analysis, or thresholding, and led to the initial inclusion of 58 cell classes, many of which were overlapping based on nomenclature and/or constituent genes. We organized cell types into seven canonical classes: microglia, endothelial cell, oligodendrocyte precursors, oligodendrocytes, astrocytes, excitatory, and inhibitory neurons. We first assigned PLS1+ significant genes to each cell type and obtained the observed counts of

overlapped genes according to the specific cell types. We then randomly selected genes with an equivalent number of a given cell type from all genes, rather than significant genes from the PLS1 gene list, and obtained the counts of overlapped genes to a given cell type [18]. These procedures were repeated 5,000 times to sample the permutation distribution of counts of overlapped genes in each cell type. The null hypothesis was that the observed count of overlapped genes (for genes assigned to each cell type) was not significantly different from the overlapped genes of a random list of genes (equivalent number of genes assigned to a given cell type). Finally, the P_{perm} values of enrichment for each cell type were estimated by comparing the observed gene counts to the centiles of null gene counts distribution for each cell type [40]. The statistical significance was set at P_{perm} < 5th or > 95th centile.

We further determined the relationships between GGE-related dysregulated genes obtained by whole-genome mRNA expression in whole blood samples and the expressions of genes related to regional MSN differences in epilepsy. The epilepsy-related dysregulated gene list was reported by Rawat *et al.* [50]. We selected 236 upregulated and 388 downregulated genes according to $P < 0.05$ after FDR correction and fold changes > 1.3. Genes used for subsequent correlation analyses were common across upregulated or downregulated genes and PLS1+ or PLS1− significant gene datasets. Robust correlation analyses [51] were used to determine relationships between PLS1+ or PLS1− significant gene weights and fold changes of upregulated or downregulated genes. The above-mentioned analyses were also used for major depressive disorder (MDD), autism spectrum disorder (ASD), schizophrenia (SCZ), bipolar disorder (BD), alcohol abuse disorder (AAD), and inflammatory bowel disease

(IBD), with diagnoses from Gandal *et al.* [52]. Because of outliers in the gene set that could potentially inflate or deflate associated correlations [18], Spearman's correlation analysis was performed to characterize the associations. We resampled the fold changes 5,000 times to test the null hypothesis that the significant association was random. The P_{perm} value was obtained from the null models (<5th or >95th centile).

Reproducibility analysis

We examined the stability and reproducibility of the regional MSN pattern using a leave-one-feature-out approach [16, 53]. We re-constructed the MSN and the regional MSN patterns using six features (one feature was removed) derived from T1w in the HC group each time. We then computed the spatial similarity (Pearson's correlation coefficient) of the regional MSN patterns between the full 7-features and 6-features. To account for spatial autocorrelation in regional MSN patterns, we obtained the statistical P_{perm} values using 5,000 spin permutation tests (see below *Spin test*). The statistical significance was set at P_{spin} < 5th or > 95th centile.

To validate the regional case-control *t*-map and minimize the effect of the participant set, the HC were divided into two subgroups HC1 (n = 75, 26 females, age: 26.09 ± 6.96 years) and HC2 (n = 75, 40 females, age: 24.67±5.79 years). One of the critical characteristics of case-control MRI data is the medication status of patients, which may influence the robustness of group analysis. To test for the robustness of the case-control *t*-map of regional MSN, patients with GGE-GTCS were divided into two subgroups: drug-experienced patients (n = 65, 21 females, age: 25.34 ± 8.09 years), and drug-naïve patients (n = 29, 12 females, age: 24.38 ± 6.47 years), whose age and

sex were matched for the HC1 and HC2 groups, respectively (all $P > 0.05$). Following the same criterion of case-control analyses, two additional abnormal patterns of regional MSN were obtained for drug-experienced patients vs. HC1 and drug-naïve patients vs. HC2. Then, correlation analyses were performed on case-control *t*-maps between drug-experienced patients vs. HC1 and all patients vs. HC, and between drug-naïve patients vs. HC2 and all patients vs. HC. Considering the overlapping sets of participants between the *t*-maps as mentioned above, we also measured the spatial similarity (Pearson's correlation coefficient) of the abnormal regional MSN between drug-experienced patients vs. HC1 and drug-naïve patients vs. HC2. The P_{spin} values were obtained by performing 5,000 spin permutation tests (<5th or >95th centile).

In addition, drug-experienced patients were divided into non-refractory (n = 49, 13 females, age: 25.73 ± 8.16 years) and refractory patients (n = 13, 7 females, age: 22.46 ± 6.32 years), whose age and sex were matched for the HC1 and HC2 groups, respectively (all $P > 0.05$). The two groups were separately compared to the HC1 and HC2 groups to obtain the case-control *t*-maps. Then, correlation analyses were performed on case-control *t*-maps between non-refractory patients vs. HC1 and all patients vs. HC, and between refractory patients vs. HC2 and all patients vs. HC. Similarly, considering the overlapping sets of participants between the *t*-maps as mentioned above, we also measured the spatial similarity (Pearson's correlation coefficient) of the abnormal regional MSN between non-refractory patients vs. HC1 and refractory patients vs. HC2. The P_{spin} values were obtained by performing 5,000 spin permutation tests (<5th or >95th centile).

To test the reproducibility of our results, we conducted a split-half analysis. Specifically, we divided the patients with GGE-GTCS into two subgroups: GGE-GTCS1 (n = 50, 12 females, age: 26.58 ± 7.99 years) and GGE-GTCS2 (n = 51, 22 females, age: 23.96 ± 7.54 years), and the age- and sex-matched HC1 and HC2, respectively (all $P > 0.05$) [5]. We performed case-control analyses of regional MSN on the subgroups (i.e., GGE-GTCS1 vs. HC1 and GGE-GTCS2 vs. HC2) regressing-out age, sex, and TIV. We then computed Pearson's correlation coefficients for the case-control *t*-maps between GGE-GTCS1 vs. HC1 and all patients vs. HC (main result), and between GGE-GTCS2 vs. HC2 and all patients vs. HC (main result). Considering the overlapping sets of participants between the above-mentioned *t*-maps, we also measured the spatial similarities (Pearson's correlation coefficient) of *t*-maps between GGE-GTCS1 vs. HC1 and GGE-GTCS2 vs. HC2. The P_{spin} values were obtained by performing 5,000 spin permutation tests (< 5th or > 95th centile).

Spin test

We used a spin-based permutation test to correct for potential confounding effects of spatial autocorrelation [36]. The spin test is a spatial permutation method based on angular permutations of spherical projections at the cortical surface. Critically, the spin test preserves the spatial covariance structure of the data and as such is far more conservative than randomly shuffling locations, which destroys the spatial covariance structure and produces an unrealistically unconservative null distribution. Specifically, we generated 5,000 random spatial rotations (i.e., spins) of the cortical regions to generate a null distribution.

Results

Analyses of samples

After quality control, acceptable T1w data were further analysed in 251 participants (Supplementary Results 1; Fig. S1) involving 101 patients with GGE-GTCS and 150 HC. Demographic and clinical characteristics are provided in Table 1. There was no significant difference in age (Mann-Whitney *U*-test, $U = 6640$, $P = 0.10$), sex ($\chi^2 = 2.69$, $P = 0.10$), TIV ($t_{(249)} = 1.22$, $P = 0.23$), or FreeSurfer's Euler number (Mann-Whitney *U*-test, $U = 6537$, $P = 0.07$; Fig. S2) between the patients and the HC. These factors were regressed out between-group comparisons. Sixty-five patients with GGE-GTCS received medication, and 29 patients were drug-naïve with newly-diagnosed GGE-GTCS. The remaining patients' clinical information was not available. In addition, 13 of 65 drug-treated patients were classified into the drug resistance group, and 49 patients were classified into the drug responsiveness group according to our previous study [13], while the drug information of three patients was unclear.

Case-control differences of regional MSN alterations

The regional MSNs showed a non-uniform distribution in both HC (Fig. 1B) and patients with GGE-GTCS (Fig. 1C), consistent with previous findings [16-18]. Specifically, highly positive MSN values were located in frontal and temporal cortical areas, and highly negative MSN values dominated in occipital and sensory-motor areas. In addition, to the best of our knowledge, we found the number of indices to construct MSN ranging from 5 to 12, which were derived from T1w or diffusion-weighted imaging or functional MRI (Supplementary Results 2; Table S1). To test the stability of the regional MSN in this study, we used the leave-one-feature-out approach to demonstrate the

spatial similarities of regional MSN among the full seven features, with one measure removed (all Pearson's *r*-values > 0.9; Fig. S3).

For case-control comparisons, by conducting a linear regression with age, sex and TIV as covariates, we found that 19 cortical regions were significantly different between the two groups (Fig. 1D). Positive and negative *t*-values denoted increased and decreased regional MSN in patients. Patients with GGE-GTCS exhibited nine increased areas in occipital, insular and posterior cingulate cortices and 10 decreased areas in prefrontal, primary motor and temporal areas (Supplementary Results 3; Table S2).

There was no significant association between the duration of illness and brain regions with significantly abnormal regional MSN values (decreased/increased, n = 19) in patients with GGE-GTCS. In addition, we performed an exploratory correlation analysis across all D-K 308 regions. We found that the insula, parahippocampal and lateral occipital cortices exhibited positive correlations with the duration of illness, whereas the parietal, postcentral, precuneus and rostral middle frontal had negative correlations with the duration of illness (Supplementary Results 4; Fig. S4). Although MSN was a valuable tool to depict abnormalities in patients, we further aimed to clarify the critical role of regional MSN patterns in patients with GGE-GTCS. We therefore used regional MSN values as features to distinguish patients with GGE-GTCS from HC [accuracy: 80.40% ± 0.53% (mean ± SD), sensitivity: 75.05% ± 0.91%, and specificity: 85.74% ± 0.69%] (Supplementary Results 5; Fig. S5).

Considering the effects of medication on the abnormal distribution of regional MSN in

patients with GGE-GTCS, we divided the patients into two subgroups, including drug-naïve and drug-treated patients. We found a consistent spatial pattern of regional MSN alterations between drug-experienced patients vs. HC1 and all patients vs. HC (Pearson's $r_{(306)}$ = 0.89, P_{spin} < 0.001; Supplementary Results 6; Fig. S6A), and between drug-naïve patients vs. HC2 and all patients vs. HC (Pearson's $r_{(306)}$ = 0.80, P_{spin} < 0.001; Fig. S6B). In addition, we found a similar spatial pattern of regional MSN alterations between drug-experienced patients vs. HC1 and drug-naïve patients vs. HC2 (Pearson's $r_{(306)}$ = 0.48, P_{spin} < 0.001; Fig. S6C), indicating the minimal effects of medication status on the main results.

After considering a previous study suggesting an association between neuroimaging and drug response [13], we repeated our analyses by classifying the drug-use patients into refractory and non-refractory groups. We found a consistent spatial pattern of regional MSN alterations between non-refractory patients vs. HC1 and all patients vs. HC (Pearson's $r_{(306)}$ = 0.85, P_{spin} < 0.001; Supplementary Results 7; Fig. S7A), between refractory patients vs. HC2 and all patients vs. HC (Pearson's $r_{(306)}$ = 0.61, P_{spin} < 0.001; Fig. S7B), and between non-refractory patients vs. HC1 and refractory patients vs. HC2 (Pearson's $r_{(306)}$ = 0.34, P_{spin} < 0.001; Fig. S7C), suggesting that the case-control regional MSN map was slightly related to variable degrees of drug response in GGE-GTCS patients. In addition, considering the small samples of refractory patients, we used the leave-one-refractory patient-out method to demonstrate the similarity of case-control *t*-maps among all refractory patients vs. HC and one refractory patients removed vs. HC (all Pearson's $r_{(306)}$ > 0.85; Fig. S8).

To test for the reproducibility of the case-control *t*-map, we conducted split-half analyses [5]. We found that the case-control *t*-maps of split-half analyses were similar between GGE-GTCS1 vs. HC1 and all patients vs. HC (Pearson's $r_{(306)} = 0.84$, $P_{spin} < 0.001$; Supplementary Results 8; Fig. S9A), and between GGE-GTCS2 vs. HC2 and all patients vs. HC (Pearson's $r_{(306)} = 0.84$, $P_{spin} < 0.001$; Fig. S9B), and between GGE-GTCS1 vs. HC1 and GGE-GTCS2 vs. HC2 (Pearson's $r_{(306)} = 0.43$, $P_{spin} < 0.001$; Fig. S9C).

To explain the case-control analysis of regional MSN at a network scale, we assigned the regions into two prior brain organizations: the Yeo-Krienen seven functional networks obtained during resting-state [54] and the von Economo cytoarchitectonic classes classified by cytoarchitectonic criteria [55]. Patients with GGE-GTCS exhibited no abnormal regions in Yeo networks (Supplementary Results 9; Table S3), and showed reduced regional MSN in von Economo class 1 (primary motor cortex, $t_{(246)} = -3.56$, $P_{FDR} = 0.003$) (Table S4; Fig. S10).

Gene expression patterns co-locate with the case-control *t*-map

The PLS1 component explained 16% variance on PLS correlation of the case-control *t*-map with gene expression (Supplementary Results 10; Fig. S11). The variance explained by the PLS1 was significantly more than expected by chance ($P = 0.02$). The weighted score of the PLS1 component is shown in Fig. 2A. In addition, we found that the PLS1 weighted gene expression map was spatially correlated with the case-control *t*-map of the regional MSN (Pearson's $r_{(150)} = 0.4$, $P_{spin} < 0.001$; Fig. 2B). We performed bootstrapping on PLS weights resulting in *Z*-scores for each gene corresponding to the PLS1 ranking. The genes were ranked according to their contributions to PLS1 (Fig. 2C).

We found 1,839 genes with normalized PLS1 weights $Z > 2.1$ and 1,723 genes with PLS1 weights $Z < -2.1$ (all $P < 0.05$, FDR corrected), such as *DGCR8*, *CACNB4* and *SLC12A5* genes.

Transcriptional enrichments for differences in regional MSN

To determine the relationships between epilepsy-related risk genes and the PLS1 significant gene list, we first generated a single omnibus gene set (119 genes) for epilepsy-related risk according to previous GWAS studies, whole-exome sequencing case-control studies, and data reported in systematic reviews [22, 23, 41-44]. After performing the multi-gene-list meta-analysis, we found that the PLS1+ significant gene set mostly shared enrichment pathways with epilepsy-related risk genes ($P < 0.05$, FDR corrected) (Fig. 3A), including "regulation of cell junction assembly", "neurotransmitter transport", "regulation of cell projection organization", "modulation of chemical synaptic transmission", "synapse organization", and "regulation of system process". In addition, the PLS1+ significant gene set obtained by the case-control *t*-map exhibited several specific enrichment pathways, including "histone modification", "chromatin organization", "protein phosphorylation", and "negative regulation of cell cycle". Visualization of intra-cluster and inter-cluster similarities of enriched terms is shown in Fig. 3B. We also found that the most interconnected pathways were located in shared enrichment pathways, such as "chemical synaptic transmission", "trans-synaptic signaling", and "synaptic signaling", which were highlighted in Fig. 3C. In addition, after using relatively restricted background genes (n = 16,831), we found that the enrichment terms were similar with the main findings. The shared pathway between epilepsy-related risk genes and PLS1+

significant genes also included “neurotransmitter transport” and “synapse organization” (Supplementary Results 11; Fig. S12). The shared pathway between epilepsy-related risk genes and PLS1− significant genes was “regulation of secretion by cell” (Fig. S13).

Enrichments at the chromosome, cell type and disease levels

We reasoned that there were transcriptional gene enrichments of MSN differences at three levels of biological complexity (from the chromosome to cell-type, and the disease level). First, regional differences were thought to be largely co-located with chromosomal genes [56]. We assessed the chromosomal enrichment of the genes using PLS1 and found that the most negatively weighted genes, which were highly expressed in decreased regions, were most strongly enriched for chromosome 11 (P_{perm} = 0.02), and chromosome 16 (P_{perm} = 0.03) genes, and the most positively weighted genes, which were highly expressed in increased regions, were most strongly enriched for chromosome 4 (P_{perm} = 0.01) and chromosome 5 (P_{perm} = 0.005) (Fig. 4A).

Second, to test the hypothesis that cellular composition was related to regional differences, we also identified specific cell types enriched for MSN alterations in our analyses. We first assigned the significant PLS1+ significant genes to seven canonical cell classes and found that a number of genes were significantly involved in excitatory neurons (number = 276, P_{perm} = 0.002), and inhibitory neurons (number = 184, P_{perm} = 0.0002) (Fig. 4B).

Finally, we found that 24 genes overlapped between the PLS1+ significant gene list and

identified genes that were significantly and differentially in whole-genome messenger RNA expressions from previous case-control studies of GGE-GTCS [50]. The PLS1+ significant gene weights were correlated with fold change values related to patients with GGE-GTCS (Spearman's $r_{s(22)}$ = –0.47, P_{perm} = 0.006; Fig. 4C). A significant correlation was not present in the six disorders described by Gandal *et al.* [52], involving: SCZ (Spearman's $r_{s(154)}$ = −0.02, P_{perm} = 0.47), ASD (Spearman's $r_{s(144)}$ = 0.01, P_{perm} = 0.49), BD (Spearman's $r_{s(23)}$ = 0.08, P_{perm} = 0.35), MDD (Spearman's $r_{s(18)}$ = –0.16, P_{perm} = 0.50), AAD (Spearman's $r_{s(32)}$ = 0.14, P_{perm} = 0.21), and IBD (Spearman's $r_{s(484)}$ = 0.06, P_{perm} = 0.07). There was no significant correlation between PLS1- gene weights and fold change values in epilepsy.

Discussion

The analysis of MSN is a novel way of assessing cortical network architecture, which has until now, not been used in patients with GGE-GTCS. Regional MSNs were significantly reduced in prefrontal and temporal areas and increased in occipital, insular and posterior cingulate cortices. By studying patterns of cortical morphometric abnormalities using multiple *in vivo* MRI parameters in relation to *ex vivo* human brain-wide transcriptional architecture, we found that the expression of genes enriched for excitatory/inhibitory neurons and chromosomes 4, 5, 11, and 16 might reflect GGE-GTCS-related MSN differences. These findings revealed MSN phenotypes in GGE and may help bridge the gap between the transcriptomes and imaging connectomes, providing an integrative understanding of the mechanisms in GGE.

MSN changes in patients with GGE-GTCS

Rather than previously used single-feature structural/morphometric approaches, the MSN approach combines information across multiple cortical features in a single participant [16, 57]. Measures of high morphological similarity may represent cytoarchitectonically similar networks that are more likely to be axonally connected to each other [16]. In addition, the MSN framework has been shown to predict inter-individual variations in human intelligence [16] and has previously helped to assess co-variations in brain morphometry and gene expressions [17-19]. We thus effectively incorporated seven cortical morphological features derived from brain MRI to differentiate patients with epilepsy using a single classification parameter [58].

In this study, we interpreted MSNs with significantly altered regions in patients with GGE-GTCS as an indication that there were decreased (or increased) architectonic similarities or more (or less) architectonic differentiation between these regions and the rest of the cortex [17, 18]. GGE-GTCS shares common morphometric brain alterations with other epilepsy subgroups and has diagnosis-specific features [8, 9, 59]. Transdiagnostic patterns of grey matter loss are located in the right thalamus, and the lower thickness is observed in the bilateral precentral gyri, parahippocampal, superior frontal, insula and caudal middle frontal cortex [8, 60]. Our observed MSN alterations were consistent with lower thickness in the precentral cortex and were consistent with reduced thickness in the precuneus and rostral middle frontal cortex and, conversely, with greater thickness in the insular cortices. Our work extended this finding by combining multiple structural indices to show that increased MSN connectivity in the insular cortex may be pathological in patients with GGE-GTCS. Replicable results might show the minimal effects of medication use and drug response on GGE-GTCS-related

MSN abnormalities. In addition, although the drug treatment group showed differences from the drug-naïve group regarding the age of onset and duration of illness, the two abnormal MSN patterns between the two groups, when compared to HC, were highly similar, indicating the minimal effect of clinical characteristics on MSN patterns.

MSN-related gene enrichment

Specific neurobiological hallmarks of MSN changes may be attributed to a host of factors such as genetic, molecular, and cellular alterations. Recently, human neuroimaging-genetic approaches have closed the gap between *in vivo* neuroimaging and its underlying molecular basis [25, 61]. Significant genes with PLS1 loading included *DGCR8*, *CACNB4*, and *SLC12A5*. These genes are protein-coding genes and are related to idiopathic generalized epilepsy [62]. Genome-wide expression profiling has revealed that protein-coding transcripts were altered in experimental and human epilepsy, including genes regulating synaptic or neuronal plasticity, cell death, proliferation, and inflammatory or immune responses [63, 64]. Heterozygous *CACNB4* variants have been implicated in epilepsy [65]. The *SLC12A5* gene encodes the neuron-specific cotransporter, K^+/Cl^- type-2, and idiopathic generalized epilepsy has been reported in patients with compound heterozygous *SLC12A5* mutations [66]. Hemizygosity for the microRNA biogenesis gene *DGCR8* leads to enhanced short- and long-term synaptic plasticity within hippocampal CA3-CA1 synapses, coinciding with spatial memory deficits [67]. We also found that shared biological and cellular processes driven from PLS1 and risk gene lists were related to “chemical synaptic transmission”, “neurotransmitter transport”, “regulation of cell projection

organization", "modulation of chemical synaptic transmission", and "synapse organization". These processes, particularly change the function of many ion channels, regulating synaptic function, and neurotransmitter receptors, and have previously been reported to contribute to epileptogenesis [68, 69]. Disturbances in synaptic transmission, in particular to the balance between excitatory and inhibitory synapses, play a role in the pathogenesis of seizures and epilepsy, and the processes of synaptic transmission are also targets for therapies for epilepsy [70]. In addition, PLS1 gene lists were specifically enriched in "histone modification", and "chromatin organization". Recent evidence has begun to elucidate the specific roles of the epigenetic mechanism, including histone code modifications and chromatin remodelling in human epilepsy syndromes, as well as the process of epileptogenesis [71]. Histone modifications play crucial roles in epilepsy and show promise in regulating chromatin structure and gene expression during epilepsy [72]. Several studies have reported alterations of histone modifications in epilepsy models [73], so these specific pathways obtained by PLS correlations suggested that transcriptome-neuroimaging analyses may provide additional information. The neuron-related terms were also enriched after using a more relatively restricted list of background genes, possibly suggesting the stability of enriched terms.

Chromosome-, cell-type- and disease-specific gene-set enrichments

To test the hypothesis that chromosomal gene expression was related to MSN changes in GGE-GTCS, we assessed chromosomal enrichment for associated genes using PLS1 [74]. We found that the most negatively and positively weighted genes, highly and lowly expressed in impacted MSN regions, were most strongly enriched for specific

chromosomes. Among patients with epilepsy, about 6% have chromosomal abnormalities, which were mainly associated with various epilepsy phenotypes and seizure types [75]. Single cases have been reported where patients with epilepsy had chromosomal abnormalities in chromosomes 4 [76] and 5 [77] associated with epilepsy. In addition, evidence suggests that people missing large amounts of DNA on chromosome 16 are more likely to develop a chronic seizure disorder during their lifetime [78]. Copy number variation of 16p13.11 has also been suggested to be a risk factor for GGE patients, even those with identically-sized 16p13.11 deletions, present with highly variable epilepsy phenotypes [79, 80]. Our data, consistent with relevant reports, highlighted the strength of our MSN analyses by confirming previously identified GGE-GTCS-related chromosomes and identifying new chromosomes [56] with relevant pathophysiological roles in patients with GGE-GTCS.

Considering the extent of cellular diversity in the brain, we need to transform normative bulk-tissue cortical expression data into cell-type expression maps [81, 82]. This will allow us to assess which cell-type-specific processes might influence selective regional vulnerabilities [83]. To this end, we took an indirect approach by assigning PLS1+ significant genes to seven canonical cell classes [18, 19, 84, 85]. We found cell type-related gene-set enrichments in excitatory and inhibitory neurons and angiogenic endothelial cells, consistent with the largest single-nucleus transcriptomic changes in distinct neuronal subtypes [86]. Target cell types in epilepsy pathophysiology create an imbalance between excitatory and inhibitory neurons but may alter integrative properties in more complex ways [87]. In addition, MSN-related transcriptomic data in endothelial cells may be associated with inflammatory and immune responses for GGE

[88]. The mechanism related to pro-inflammatory expression may involve the regulation of the innate immune reaction in response to seizures [50, 69, 89]. Taken together, excitatory neurons and inhibitory neurons may contribute to the generation of epileptic seizures and immune responses in epilepsy pathogenesis.

We also found that 24 genes overlapped between the PLS1+ significant gene list and the significantly differentially expressed genes (DEGs) in peripheral blood mRNA from case-control studies of GGE patients. These PLS1+ gene weights were correlated with GGE-related upregulated DEGs, but there was no correlation between PLS1+ gene weights and five disease-related DEGs from case-control post-mortem brain tissue [52]. These findings suggested a degree of specificity across diagnostic groups and transcriptional correlates of GGE-related changes in MSN capturing patterns of gene upregulation. Collectively, the identified GGE-related chromosomes, cell types and disease-related gene-set enrichments verified the validity of gene ranks obtained from changes in MSN and enabled us to identify potential biological targets of GGE-GTCS.

Methodological considerations

Several methodological issues had to be considered. First, the medication for drug-experienced patients were heterogeneous. There were more than 10 types of medication for drug-experienced patients. In addition, at least 13 drug-experienced patients were treated with more than two types of drugs. Therefore, we could not identify the effects of medication type on the case-control *t*-map. Future investigations should control the medication type for patients to solve this issue, and it may be more appropriate to sub-stratify according to the type of medication, e.g., 6 months prior to

examination. Second, we did not have access to the molecular characteristics of our samples, limiting the ability to determine the direct effects of genetic variations on abnormal patterns of regional MSNs. Third, the AHBA dataset was only based on six participants and only included data for the right hemisphere for two of them. Differences in sample characteristics, for example, between the AHBA donors and the participants of our Chinese neuroimaging study, may furthermore require additional caution in interpreting imaging-genetic findings. Finally, because the significant genes were not identified based on correlations with spatially-defined phenotypes, but obtained by PLS correlation analyses, the newly proposed strategy [90] that mitigates the bias of leveraging gene enrichment approach in the spatial transcriptomic data could not be directly used [91]. In addition, we used a multi-gene-list meta-analysis to identify the shared and specific pathways between GGE-related risk genes from GWAS and PLS1 significant genes, which could not be performed by the newly proposed strategy [90]. Future studies will hopefully develop methods to test the effects of this type of bias on the present results.

Conclusions

In summary, we showed that patients with GGE-GTCS had altered regional MSNs, mainly observed in the prefrontal, temporal, and occipital cortices, which provided a better understanding of the potential mechanisms of GGE-GTCS pathophysiology. By correlating our neuroimaging findings to post-mortem transcriptomics, we found that regional MSN changes in patients with GGE-GTCS were associated with genes expressed across distinct chromosomes and cellular types. Our findings highlight the importance of bridging diverse types of biological organization when studying brain

dysfunction.

Conflict of interest

The authors declare no competing interests.

Acknowledgements

We are grateful to all the participants in this study. We thank International Science Editing (http://www.internationalscienceediting.com) for editing this manuscript. This work was supported by the National Key Project of Research and Development of the Ministry of Science and Technology (2022YFC2009900 and 2022YFC2009906), National Natural Science Foundation of China (82202250, 61871077, 62036003, U1808204, and 81871345), the Excellent Youth Foundation of Sichuan Scientific Committee (2020JDJQ0016), the China Postdoctoral Science Foundation (BX2021057 and 2022M710615).

Author contributions

W.L., Z.Z. and H.C. led the project. J.L., W.L., Z.Z., and H.C. were responsible for the study concept and the design of the study. B.L. and J.S. analysed the transcriptional data. S.K. and B.B. made substantial contributions to the manuscript and provided critical comments. Y.W., Y.M., and S.Y. analysed neuroimaging data and checked the imaging quality. Q.X., Q.Z., F.Y., and G.L. collected the neuroimaging data. J.L. and W.L. created the figures and wrote the manuscript. All authors reviewed and commented on the manuscript.

Data availability

Human gene expression data that support the findings of this study are available in the Allen Brain Atlas ("Complete normalized microarray datasets", https://human.brainmap.org/static/download). The PLS1 significant gene list is provided in Dataset S1. The background gene list is provided in Dataset S2. Epilepsy-related risk genes can be obtained from previous GWAS studies using either meta- and mega-analysis or whole-exome sequencing, and systematic reviews [22, 23, 41-44]. Differential genes expression values of epilepsy and other brain disorders are from the raw Rawat et al. [50] (https://ars.els-cdn.com/content/image/1-s2.0-S0888754318305093-mmc3.xlsx) and Gandal et al. (https://www.ncbi.nlm.nih.gov/pmc/articles/PMC5898828/#SD1) datasets, respectively. Compiled cell-specific gene set list can be obtained from the raw Seidlitz et al. [19] dataset (https://staticcontent.springer.com/esm/art%3A10.1038%2Fs41467-020-17051-5/MediaObjects/41467_2020_17051_MOESM8_ESM.xlsx).

References

1. Thijs RD, Surges R, O'Brien TJ, Sander JW. Epilepsy in adults. Lancet 2019;393:689-701.
2. Fisher RS, Cross JH, French JA, et al. Operational classification of seizure types by the International League Against Epilepsy: Position Paper of the ILAE Commission for Classification and Terminology. Epilepsia 2017;58:522-530.
3. Mullen SA, Berkovic SF. Genetic generalized epilepsies. Epilepsia 2018;59:1148-1153.
4. Wang Z, Lariviere S, Xu Q, et al. Community-informed connectomics of the thalamocortical system in generalized epilepsy. Neurology 2019;93:e1112-e1122.
5. Zhang Z, Liao W, Chen H, et al. Altered functional-structural coupling of large-scale brain networks in idiopathic generalized epilepsy. Brain 2011;134:2912-2928.
6. Liao W, Zhang Z, Pan Z, et al. Altered functional connectivity and small-world in mesial temporal lobe epilepsy. PLoS One 2010;5:e8525.
7. Bernhardt BC, Rozen DA, Worsley KJ, et al. Thalamo-cortical network pathology in idiopathic generalized epilepsy: insights from MRI-based morphometric correlation analysis. Neuroimage 2009;46:373-381.
8. Whelan CD, Altmann A, Botia JA, et al. Structural brain abnormalities in the common epilepsies assessed in a worldwide ENIGMA study. Brain 2018;141:391-408.
9. Lariviere S, Rodriguez-Cruces R, Royer J, et al. Network-based atrophy modeling in the common epilepsies: A worldwide ENIGMA study. Sci Adv 2020;6:eabc6457.
10. Yang S, Zhang Z, Chen H, et al. Temporal variability profiling of the default mode across epilepsy subtypes. Epilepsia 2021;62:61-73.
11. Meng Y, Yang S, Chen H, et al. Systematically disrupted functional gradient of the cortical connectome in generalized epilepsy: Initial discovery and independent sample replication. Neuroimage 2021;230:117831.
12. Bin G, Wang T, Zeng H, et al. Patterns of gray matter abnormalities in idiopathic generalized epilepsy: a meta-analysis of voxel-based morphology studies. PLoS One 2017;12:e0169076.
13. Weng Y, Lariviere S, Caciagli L, et al. Macroscale and microcircuit dissociation of focal and generalized human epilepsies. Commun Biol 2020;3:244.
14. Nuyts S, D'Souza W, Bowden SC, Vogrin SJ. Structural brain abnormalities in genetic generalized epilepsies: a systematic review and meta-analysis. Epilepsia 2017;58:2025-2037.
15. Bernasconi N, Wang I. Emerging Trends in Neuroimaging of Epilepsy. Epilepsy Curr 2021;21:79-82.
16. Seidlitz J, Vasa F, Shinn M, et al. Morphometric similarity networks detect microscale cortical organization and predict inter-individual cognitive variation. Neuron 2018;97:231-247 e237.
17. Morgan SE, Seidlitz J, Whitaker KJ, et al. Cortical patterning of abnormal morphometric similarity in psychosis is associated with brain expression of schizophrenia-related genes. Proc Natl Acad Sci U S A 2019;116:9604-9609.
18. Li J, Seidlitz J, Suckling J, et al. Cortical structural differences in major depressive

disorder correlate with cell type-specific transcriptional signatures. Nat Commun 2021;12:1647.
19. Seidlitz J, Nadig A, Liu S, et al. Transcriptomic and cellular decoding of regional brain vulnerability to neurogenetic disorders. Nat Commun 2020;11:3358.
20. Speed D, O'Brien TJ, Palotie A, et al. Describing the genetic architecture of epilepsy through heritability analysis. Brain 2014;137:2680-2689.
21. Ellis CA, Ottman R, Epstein MP, Berkovic SF. Generalized, focal, and combined epilepsies in families: new evidence for distinct genetic factors. Epilepsia 2020;61:2667-2674.
22. Epilepsies ILAECoC. Genetic determinants of common epilepsies: a meta-analysis of genome-wide association studies. Lancet Neurol 2014;13:893-903.
23. Epilepsies ILAECoC. Genome-wide mega-analysis identifies 16 loci and highlights diverse biological mechanisms in the common epilepsies. Nat Commun 2018;9:5269.
24. Hawrylycz MJ, Lein ES, Guillozet-Bongaarts AL, et al. An anatomically comprehensive atlas of the adult human brain transcriptome. Nature 2012;489:391-399.
25. Fornito A, Arnatkeviciute A, Fulcher BD. Bridging the gap between connectome and transcriptome. Trends Cogn Sci 2019;23:34-50.
26. de Bézenac CE, Caciagli L, Alonazi BK, et al. Altered functional connectome hierarchy with gene expression signatures in newly-diagnosed focal epilepsy. medRxiv 2021;DOI: 10.1101/2021.07.18.21259977.
27. Park BY, Hong SJ, Valk SL, et al. Differences in subcortico-cortical interactions identified from connectome and microcircuit models in autism. Nat Commun 2021;12:2225.
28. Altmann A, Ryten M, Nunzio MD, et al. A systems-level analysis highlights microglial activation as a modifying factor in common forms of human epilepsy. Neuropathol Appl Neurobiol 2021;In press:doi.org/10.1111/nan.12758.
29. Howard DM, Adams MJ, Clarke TK, et al. Genome-wide meta-analysis of depression identifies 102 independent variants and highlights the importance of the prefrontal brain regions. Nat Neurosci 2019;22:343-352.
30. Dale AM, Fischl B, Sereno MI. Cortical surface-based analysis. I. Segmentation and surface reconstruction. Neuroimage 1999;9:179-194.
31. Romero-Garcia R, Atienza M, Clemmensen LH, Cantero JL. Effects of network resolution on topological properties of human neocortex. Neuroimage 2012;59:3522-3532.
32. Desikan RS, Segonne F, Fischl B, et al. An automated labeling system for subdividing the human cerebral cortex on MRI scans into gyral based regions of interest. Neuroimage 2006;31:968-980.
33. Whitaker KJ, Vertes PE, Romero-Garcia R, et al. Adolescence is associated with genomically patterned consolidation of the hubs of the human brain connectome. Proc Natl Acad Sci U S A 2016;113:9105-9110.
34. Arnatkeviciute A, Fulcher BD, Fornito A. A practical guide to linking brain-wide gene expression and neuroimaging data. Neuroimage 2019;189:353-367.
35. Krishnan A, Williams LJ, McIntosh AR, Abdi H. Partial Least Squares (PLS)

methods for neuroimaging: a tutorial and review. Neuroimage 2011;56:455-475.
36. Vasa F, Seidlitz J, Romero-Garcia R, et al. Adolescent tuning of association cortex in human structural brain networks. Cereb Cortex 2018;28:281-294.
37. Alexander-Bloch AF, Shou H, Liu S, et al. On testing for spatial correspondence between maps of human brain structure and function. Neuroimage 2018;178:540-551.
38. Li J, Wu GR, Li B, et al. Transcriptomic and macroscopic architectures of intersubject functional variability in human brain white-matter. Commun Biol 2021;4:1417.
39. Dorfschmidt L, Bethlehem RA, Seidlitz J, et al. Sexually divergent development of depression-related brain networks during healthy human adolescence. Sci Adv 2022;8:eabm7825.
40. Romero-Garcia R, Seidlitz J, Whitaker KJ, et al. Schizotypy-related magnetization of cortex in healthy adolescence is colocated with expression of schizophrenia-related genes. Biol Psychiatry 2020;88:248-259.
41. consortium EK. Ultra-rare genetic variation in common epilepsies: a case-control sequencing study. Lancet Neurol 2017;16:135-143.
42. May P, Girard S, Harrer M, et al. Rare coding variants in genes encoding GABAA receptors in genetic generalised epilepsies: an exome-based case-control study. Lancet Neurol 2018;17:699-708.
43. Collaborative E. Ultra-rare genetic variation in the epilepsies: a whole-exome sequencing study of 17,606 individuals. Am J Hum Genet 2019;105:267-282.
44. Consortium E. A roadmap for precision medicine in the epilepsies. Lancet Neurol 2015;14:1219-1228.
45. Zhou Y, Zhou B, Pache L, et al. Metascape provides a biologist-oriented resource for the analysis of systems-level datasets. Nat Commun 2019;10:1523.
46. Evangelou E, Ioannidis JP. Meta-analysis methods for genome-wide association studies and beyond. Nat Rev Genet 2013;14:379-389.
47. Liberali P, Snijder B, Pelkmans L. Single-cell and multivariate approaches in genetic perturbation screens. Nat Rev Genet 2015;16:18-32.
48. Arloth J, Bader DM, Roh S, Altmann A. Re-annotator: annotation pipeline for microarray probe sequences. PLoS One 2015;10:e0139516.
49. Benjamini Y, Hochberg Y. Controlling the false discovery rate—a practical and powerful approach to multiple testing. R Stat Soc Series B Stat Methodol 1995;57:289-300.
50. Rawat C, Kushwaha S, Srivastava AK, Kukreti R. Peripheral blood gene expression signatures associated with epilepsy and its etiologic classification. Genomics 2020;112:218-224.
51. Pernet CR, Wilcox R, Rousselet GA. Robust correlation analyses: false positive and power validation using a new open source matlab toolbox. Front Psychol 2012;3:606.
52. Gandal MJ, Haney JR, Parikshak NN, et al. Shared molecular neuropathology across major psychiatric disorders parallels polygenic overlap. Science 2018;359:693-697.
53. Yang S, Wagstyl K, Meng Y, et al. Cortical patterning of morphometric similarity

gradient reveals diverged hierarchical organization in sensory-motor cortices. Cell Rep 2021;36:109582.
54. Yeo BT, Krienen FM, Sepulcre J, et al. The organization of the human cerebral cortex estimated by intrinsic functional connectivity. J Neurophysiol 2011;106:1125-1165.
55. von Economo C, Koskinas GN. *Atlas of Cytoarchitectonics of the Adult Human Cerebral Cortex*. S Karger AG, 2008.
56. Singh R, Gardner RJ, Crossland KM, Scheffer IE, Berkovic SF. Chromosomal abnormalities and epilepsy: a review for clinicians and gene hunters. Epilepsia 2002;43:127-140.
57. Wei YB, Scholtens LH, Turk E, van den Heuvel MP. Multiscale examination of cytoarchitectonic similarity and human brain connectivity. Netw Neurosci 2019;3:124-137.
58. Lai C, Guo S, Cheng L, Wang W. A comparative study of feature selection methods for the discriminative analysis of temporal lobe epilepsy. Front Neurol 2017;8:633.
59. Sisodiya SM, Whelan CD, Hatton SN, et al. The ENIGMA-Epilepsy working group: mapping disease from large data sets. Hum Brain Mapp 2020;In press:https://doi.org/10.1002/hbm.25037.
60. Park KM, Kim SE, Lee BI, Hur YJ. Brain morphology in patients with genetic generalized epilepsy: its heterogeneity among subsyndromes. Eur Neurol 2018;80:236-244.
61. Richiardi J, Altmann A, Milazzo AC, et al. BRAIN NETWORKS. Correlated gene expression supports synchronous activity in brain networks. Science 2015;348:1241-1244.
62. Wang J, Lin ZJ, Liu L, et al. Epilepsy-associated genes. Seizure 2017;44:11-20.
63. Pitkanen A, Lukasiuk K. Mechanisms of epileptogenesis and potential treatment targets. Lancet Neurol 2011;10:173-186.
64. Miller-Delaney SF, Bryan K, Das S, et al. Differential DNA methylation profiles of coding and non-coding genes define hippocampal sclerosis in human temporal lobe epilepsy. Brain 2015;138:616-631.
65. Coste de Bagneaux P, von Elsner L, Bierhals T, et al. A homozygous missense variant in CACNB4 encoding the auxiliary calcium channel beta4 subunit causes a severe neurodevelopmental disorder and impairs channel and non-channel functions. PLoS Genet 2020;16:e1008625.
66. Martinez LA, Lai YC, Holder JL, Jr., Anderson AE. Genetics in Epilepsy. Neurol Clin 2021;39:743-777.
67. Eaton CB, Thomas RH, Hamandi K, et al. Epilepsy and seizures in young people with 22q11.2 deletion syndrome: prevalence and links with other neurodevelopmental disorders. Epilepsia 2019;60:818-829.
68. Ellis CA, Petrovski S, Berkovic SF. Epilepsy genetics: clinical impacts and biological insights. Lancet Neurol 2020;19:93-100.
69. Jin Y, Zhao C, Chen L, et al. Identification of novel gene and pathway targets for human epilepsy treatment. Biol Res 2016;49:3.
70. Casillas-Espinosa PM, Powell KL, O'Brien TJ. Regulators of synaptic transmission:

roles in the pathogenesis and treatment of epilepsy. Epilepsia 2012;53 Suppl 9:41-58.
71. Qureshi IA, Mehler MF. Epigenetic mechanisms underlying human epileptic disorders and the process of epileptogenesis. Neurobiol Dis 2010;39:53-60.
72. Hauser RM, Henshall DC, Lubin FD. The Epigenetics of Epilepsy and Its Progression. Neuroscientist 2018;24:186-200.
73. Conboy K, Henshall DC, Brennan GP. Epigenetic principles underlying epileptogenesis and epilepsy syndromes. Neurobiol Dis 2021;148:105179.
74. Liu S, Seidlitz J, Blumenthal JD, Clasen LS, Raznahan A. Integrative structural, functional, and transcriptomic analyses of sex-biased brain organization in humans. Proc Natl Acad Sci U S A 2020;117:18788-18798.
75. Specchio N, Carotenuto A, Trivisano M, et al. Ring 21 chromosome presenting with epilepsy and intellectual disability: clinical report and review of the literature. Am J Med Genet A 2011;155A:911-914.
76. Soysal Y, Balci S, Hekimler K, et al. Characterization of double ring chromosome 4 mosaicism associated with bilateral hip dislocation, cortical dysgenesis, and epilepsy. Am J Med Genet A 2009;149A:2782-2787.
77. Kluger G, Koehler U, Neuhann TM, et al. Generalized epilepsy in two patients with 5p duplication. Neuropediatrics 2013;44:225-229.
78. DUMCC. Rare gene variants linked to high risk of broad range of seizure disorders. North Carolina, United States: ScienceDaily, 2010.
79. Thomas RH, Berkovic SF. The hidden genetics of epilepsy-a clinically important new paradigm. Nat Rev Neurol 2014;10:283-292.
80. de Kovel CG, Trucks H, Helbig I, et al. Recurrent microdeletions at 15q11.2 and 16p13.11 predispose to idiopathic generalized epilepsies. Brain 2010;133:23-32.
81. Lake BB, Chen S, Sos BC, et al. Integrative single-cell analysis of transcriptional and epigenetic states in the human adult brain. Nat Biotechnol 2018;36:70-80.
82. Li MF, Santpere G, Kawasawa YI, et al. Integrative functional genomic analysis of human brain development and neuropsychiatric risks. Science 2018;362:eaat7615.
83. Diez I, Sepulcre J. Unveiling the neuroimaging-genetic intersections in the human brain. Curr Opin Neurol 2021;34:480-487.
84. Anderson KM, Collins MA, Kong R, et al. Convergent molecular, cellular, and cortical neuroimaging signatures of major depressive disorder. Proc Natl Acad Sci U S A 2020;117:25138-25149.
85. Hansen JY, Markello RD, Vogel JW, et al. Mapping gene transcription and neurocognition across human neocortex. Nat Hum Behav 2021;5:1240-1250.
86. Pfisterer U, Petukhov V, Demharter S, et al. Identification of epilepsy-associated neuronal subtypes and gene expression underlying epileptogenesis. Nat Commun 2020;11:5038.
87. Noebels JL. The biology of epilepsy genes. Annu Rev Neurosci 2003;26:599-625.
88. Vezzani A, French J, Bartfai T, Baram TZ. The role of inflammation in epilepsy. Nat Rev Neurol 2011;7:31-40.
89. Turrin NP, Rivest S. Innate immune reaction in response to seizures: implications for the neuropathology associated with epilepsy. Neurobiol Dis 2004;16:321-334.
90. Fulcher BD, Arnatkeviciute A, Fornito A. Overcoming false-positive gene-

category enrichment in the analysis of spatially resolved transcriptomic brain atlas data. Nat Commun 2021;12:2669.
91. Wang Y, Chai L, Chu C, et al. Uncovering the genetic profiles underlying the intrinsic organization of the human cerebellum. Mol Psychiatry 2022;27:2619-2634.

Tables

Table 1. Clinical and Demographic Characteristics.

Variables	GGE-GTCS (n = 101)	HC (n = 150)	Statistics (GGE-GTCS vs. HC)
Age at scan (years)	25.26 ± 7.84	25.38 ± 6.42	U = 6640, P = 0.10
Sex (female/male)	34/67	66/84	χ^2 = 2.69, P = 0.10
Handedness (left/right)	0/101	0/150	χ^2 = 0, P =1
Duration of illness (months)	69.52 ± 86.33	N.A.	N.A.
Onset age (years)	19.46 ± 8.81	N.A.	N.A.
Medication (yes/no)	65/29	N.A.	N.A.
Refractory (yes/no)	13/49	N.A.	N.A.

Note: Data are presented as either n or means ± standard deviations. The cohort size was obtained after the image data quality control.

Abbreviations: GGE-GTCS, genetic generalized epilepsy with generalized tonic-clonic seizures; HC, healthy controls; N.A., not available.

The U value was obtained by Mann–Whitney U–test (two-sided). The χ^2 values were obtained by Chi-square test.

Figures

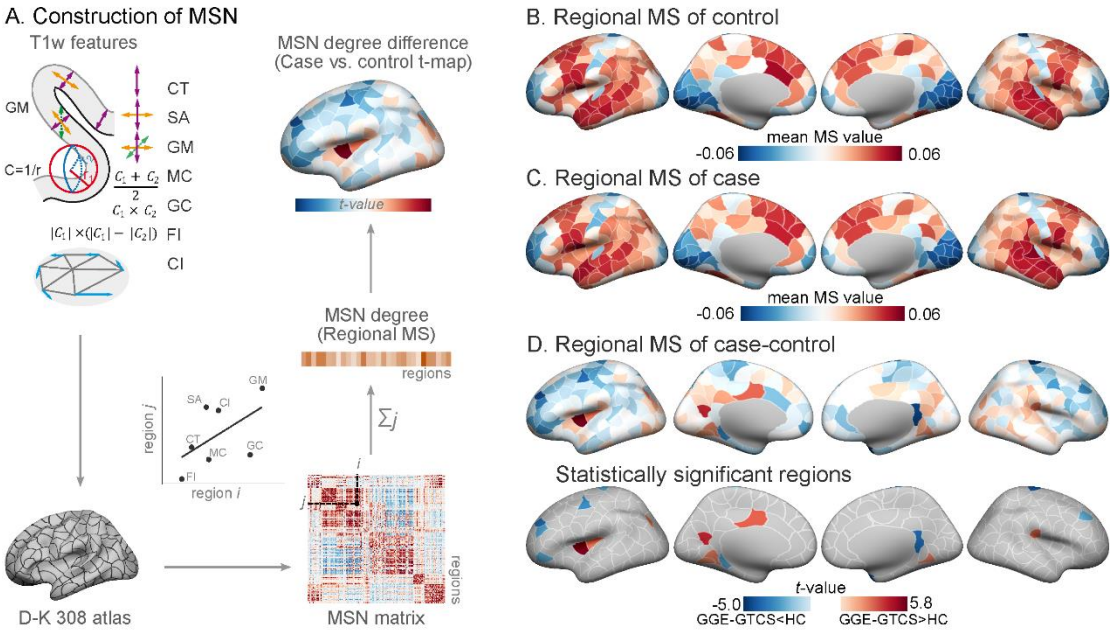

Figure 1. Case-control differences in regional morphometric similarity networks (MSN). (A) Flow chart of the construction of the regional MSN. Pearson's correlation coefficient was used to analyse morphometric features between each paired region including surface area (SA), cortical thickness (CT), grey matter volume (GMV), intrinsic Gaussian curvature (GC), mean curvature (MC), curved index (CI), and folding index (FI). (B) Mean regional MSN values across healthy controls. Highly positive morphometric similarities were located in the frontal and temporal cortical areas; whereases highly negative MSN were located in occipital and sensory-motor areas. (C) Mean regional MSN values across patients with genetic generalized epilepsy with generalized tonic-clonic seizures. (D) Case-control t-map of regional MSN. Nineteen cortical regions showed statistically significant differences ($P < 0.05$, false-discovery rate-corrected).

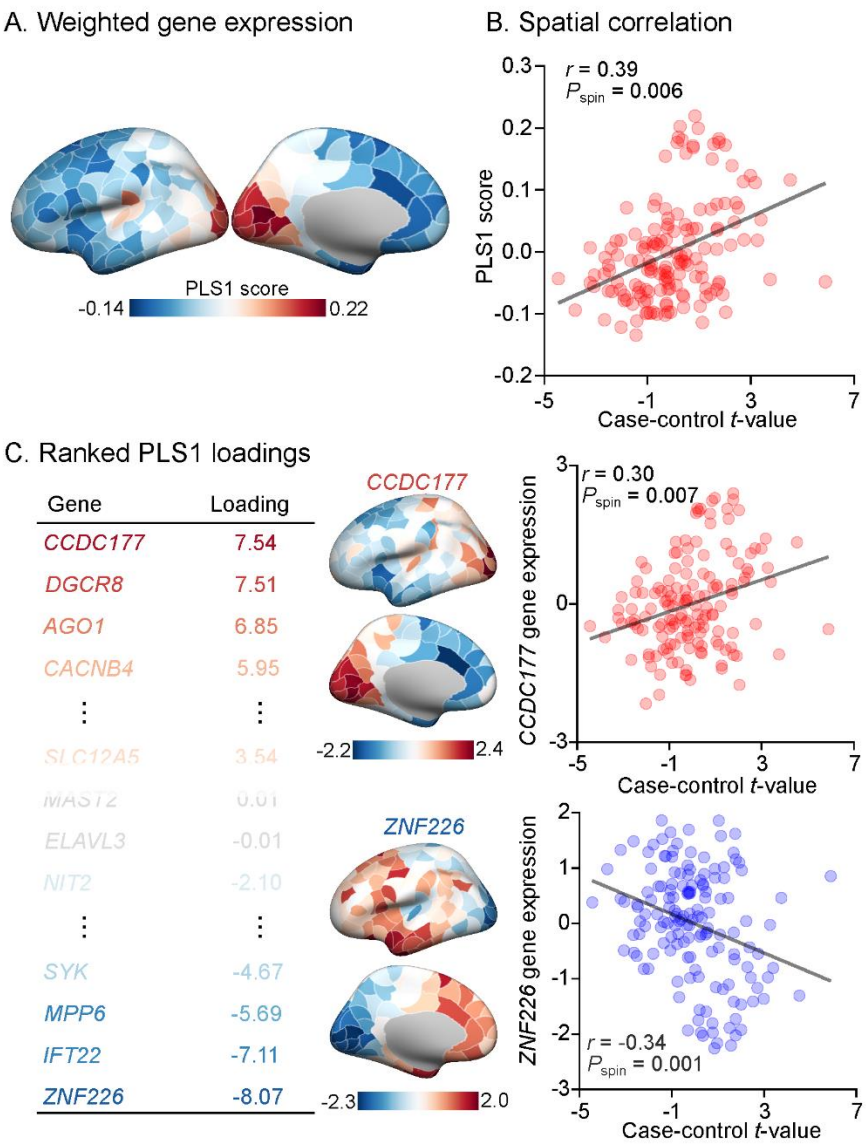

Figure 2. Gene expression profiles related to the case-control *t*-map of regional morphometric similarities networks (MSN). (**A**) A weighted gene expression map of the first component of partial least square (PLS1) in the left hemisphere. (**B**) A scatterplot of regional PLS1 scores and case-control t-values of regional MSN (Pearson's $r_{(150)}$ = 0.39, P_{spin} = 0.006). (**C**) Ranked PLS1 loadings. Genes that were strongly positively weighted on PLS1 (e.g., *CCDC177*) positively correlated with case-control *t*-maps of regional MSN (r = 0.30, P_{spin} = 0.007), whereas genes that were strongly negatively weighted on PLS1 (e.g., *ZNF226*) negatively correlated with case-control *t*-maps of regional MSN (r = -0.34, P_{spin} = 0.001).

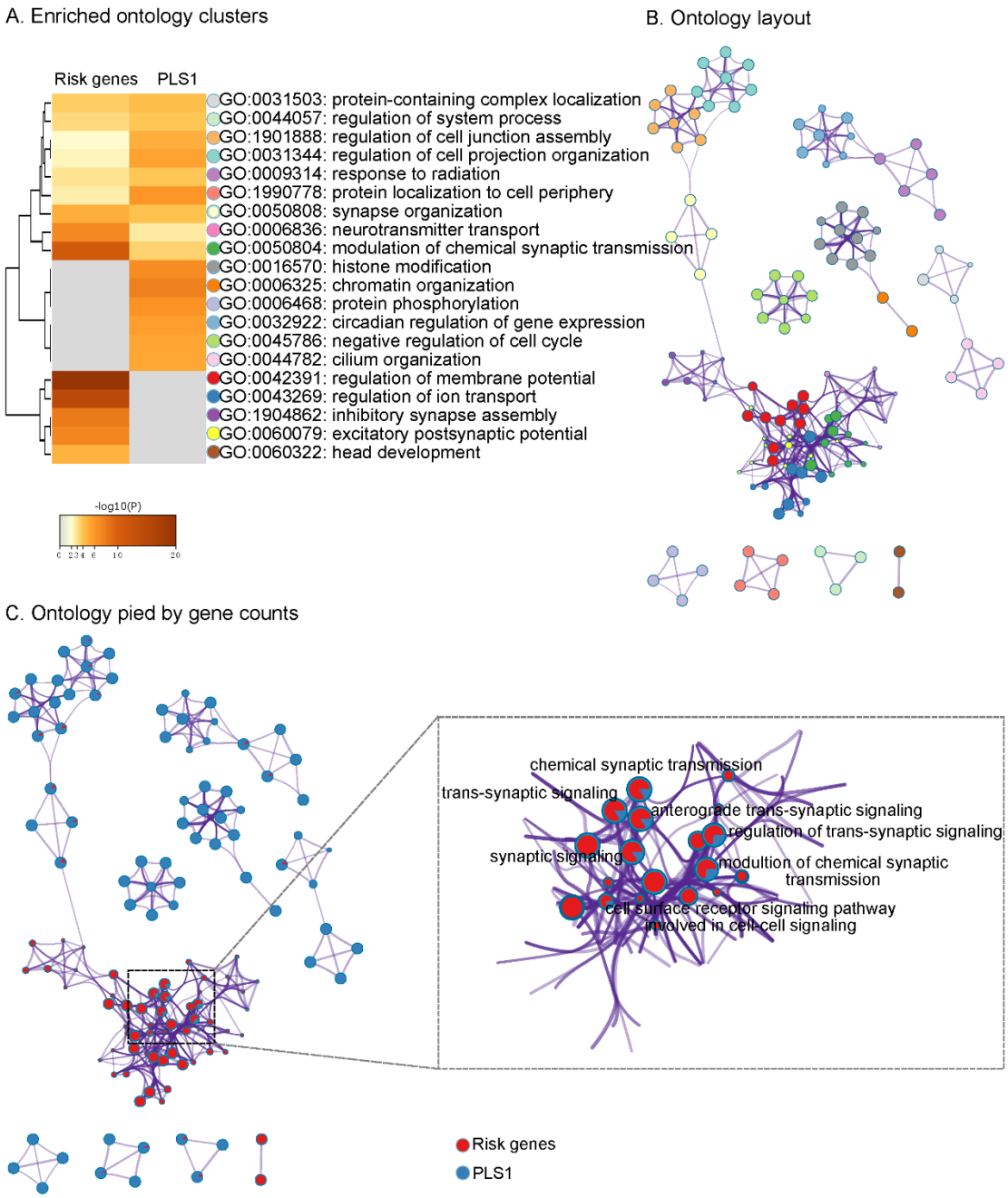

Figure 3. Functional enrichments of gene transcripts. (**A**) Gene ontology terms enriched for differences in the regional morphometric similarity network (MSN)-related PLS1+ significant genes and epilepsy-related risk genes from previous genome-wide association studies using either meta- and mega-analysis or whole-exome sequencing, and systematic reviews. (**B**) A subset of representative ontology terms from all enriched clusters (P < 0.05, false-discovery rate corrected). (**C**) The same enrichment network with its nodes is displayed as pie sections. Each pie sector is

proportional to the number of hits originating from a gene list. Red colour represents the ontology terms for risk genes, and blue colour represents the functional enrichments obtained by PLS1+ significant genes. The most interconnected pathways and the same enriched pathways between risk genes and PLS1+ significant genes are highlighted, such as “chemical synaptic transmission” and “synaptic signaling”.

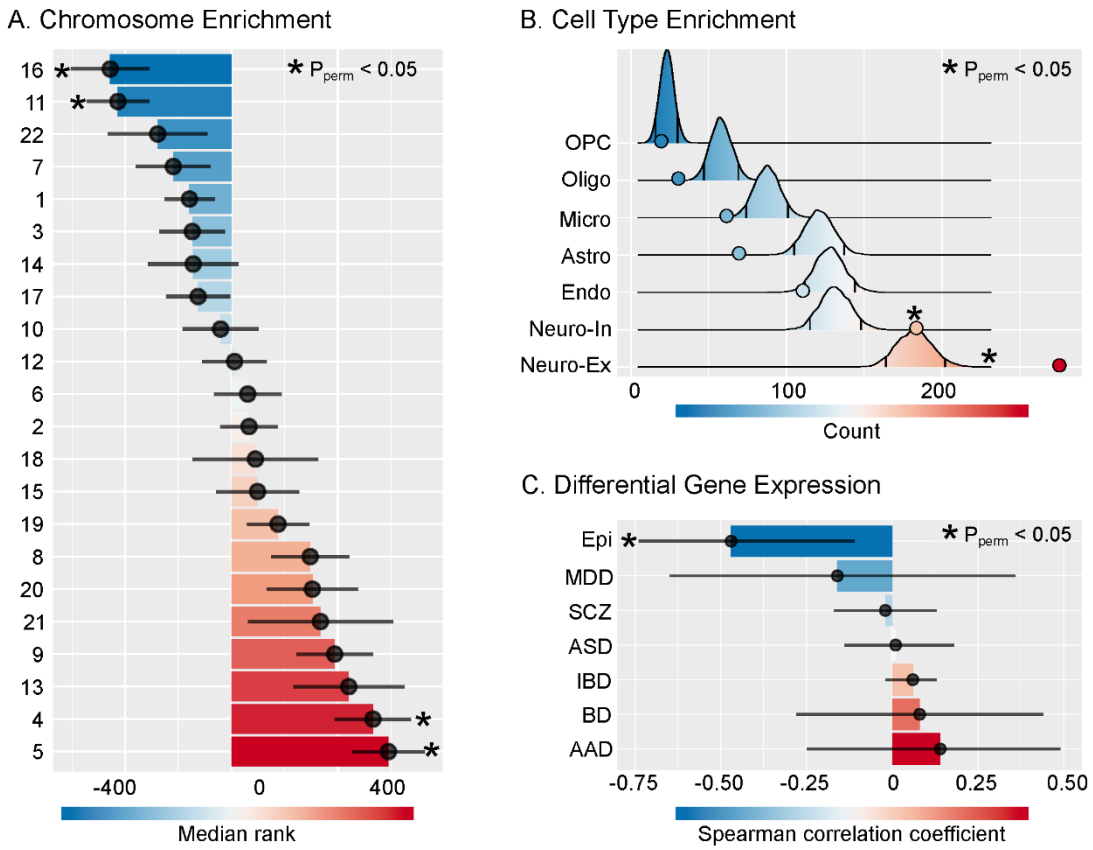

Figure 4. Chromosome-, cell-types-, and epilepsy-related specific expression relationships to changes in the morphometric similarity network (MSN)-related genes. (**A**) Enrichment analysis for chromosomal genes. A plot of the median rank of genes from each chromosome on PLS1 with standard deviations. (**B**) Enrichment analysis for cell-types-specific genes. Significantly weighted genes were enriched in genes expressed by excitatory neurons and inhibitory neurons. (**C**) Enrichment analysis for epilepsy-related genes and other disorders-related genes. The PLS1+ significant weighed gene expression was associated with downregulated differential gene expression in epilepsy (Spearman's $r_{s(22)}$ = –0.47, P_{perm} = 0.006). However, this association was not found in the other disorders. An asterisk represents $P_{perm} < 0.05$.